Research Article
doi.org/10.1002/chem.202200394

www.chemeurj.org

Strong Antibiotic Activity of the Myxocoumarin Scaffold *in vitro* and *in vivo*

Gesa Hertrampf,[a] Kalina Kusserow,[b] Sandra Vojnovic,[c] Aleksandar Pavic,[c] Jonas I. Müller,[a] Jasmina Nikodinovic-Runic,*[c] and Tobias A. M. Gulder*[a]

Abstract: The increasing emergence of resistances against established antibiotics is a substantial threat to human health. The discovery of new compounds with potent antibiotic activity is thus of utmost importance. Within this work, we identify strong antibiotic activity of the natural product myxocoumarin B from *Stigmatella aurantiaca* MYX-030 against a range of clinically relevant bacterial pathogens, including clinical isolates of MRSA. A focused library of structural analogs was synthesized to explore initial structure-activity relationships and to identify equipotent myxocoumarin derivatives devoid of the natural nitro substituent to significantly streamline synthetic access. The cytotoxicity of the myxocoumarins as well as their potential to cure bacterial infections *in vivo* was established using a zebrafish model system. Our results reveal the exceptional antibiotic activity of the myxocoumarin scaffold and hence its potential for the development of novel antibiotics.

Myxobacteria are talented producers of complex, biomedically interesting specialized metabolites from most diverse natural product classes.[1] Prominent examples include epothilone A (**1**) and analogs as anti-cancer chemotherapeutics,[2] the antifungal soraphen $A_{1\alpha}$ (**2**),[3] or the antibacterial cystobactamids,[4] such as **3** (Figure 1). These organisms have thus proven to be a promising resource for the discovery of new small molecules with potent biological functions, particularly for applications with increasing demand due to emerging resistance against currently known agents, both in the agrochemical and medical sectors. In 2013, we have described the discovery of two natural products from *Stigmatella aurantiaca* MYX-030, myxocoumarins A (**4**) and B (**5**), both of which being equipped with a long alkyl side chain and a rare aromatic nitro group.[5] Myxocoumarin A (**4**) displayed potent inhibitory effects against a range of agrochemically relevant pathogenic fungi, while **5** could not be biologically assessed due to the low production titers and the loss of a viable producing strain. To allow for antifungal evaluation of **5**, a concise total synthesis of this compound was developed, revealing a complete lack of the anticipated antifungal properties.[6] A possible natural function as well as

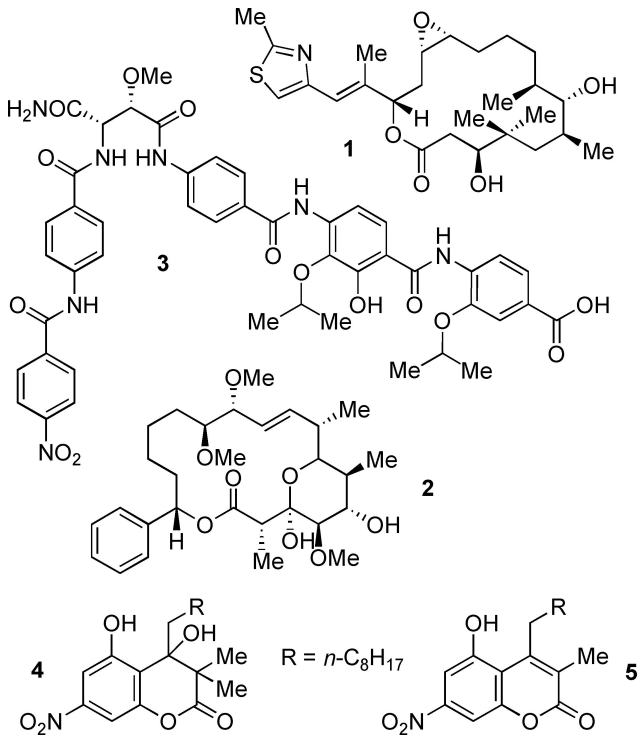

Figure 1. Chemical structures of the myxobacterial natural products epothilone A (**1**), soraphen $A_{1\alpha}$ (**2**), cystobactamide **3** and the myxocoumarins A (**4**) and B (**5**).

[a] *G. Hertrampf,+ J. I. Müller, Prof. Dr. T. A. M. Gulder*
Chair of Technical Biochemistry
Technical University of Dresden
Bergstraße 66, 01069 Dresden (Germany)
E-mail: tobias.gulder@tu-dresden.de

[b] *Dr. K. Kusserow+*
Biosystems Chemistry
Technical University of Munich
Lichtenbergstraße 4, 85748 Garching bei München (Germany)

[c] *Dr. S. Vojnovic, Dr. A. Pavic, Dr. J. Nikodinovic-Runic*
Institute of Molecular Genetics and Genetic Engineering
University of Belgrade
Vojvode Stepe 444a, Belgrade, 11000 (Serbia)
E-mail: jasmina.nikodinovic@gmail.com
jasmina.nikodinovic@imgge.bg.ac.rs

Supporting information for this article is available on the WWW under https://doi.org/10.1002/chem.202200394

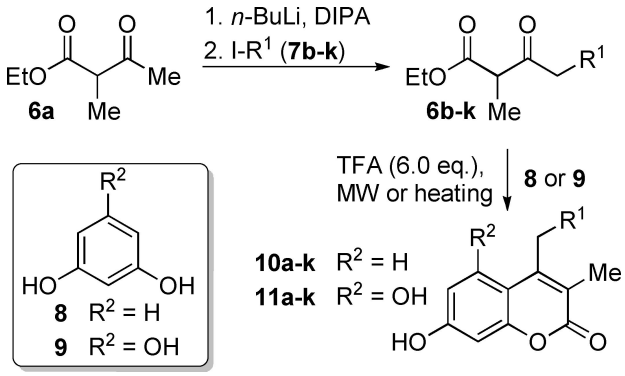

Scheme 1. Synthesis of hydroxy-substituted myxocoumarin analogs **10a–k** and **11a–k** by Pechmann condensation with β-keto esters **6a–k** with different side-chains R^1.

Table 1. Substitution pattern and synthetic yields of analogs **10** and **11**.

Compound	R^1	Yield [%] of **10** (R^2 = H)	Yield [%] of **11** (R^2 = OH)
a	H	69	73
b	*n*-C_3	42	30
c	*n*-C_4	42	33
d	*n*-C_5	26	27
e	*n*-C_6	36	32
f	*n*-C_7	35	25
g	*n*-C_8	33	42
h	*n*-C_9	30	25
i	*n*-C_{10}	30	26
j	*n*-C_{12}	25	28
k	*iso*-C_5	37	19

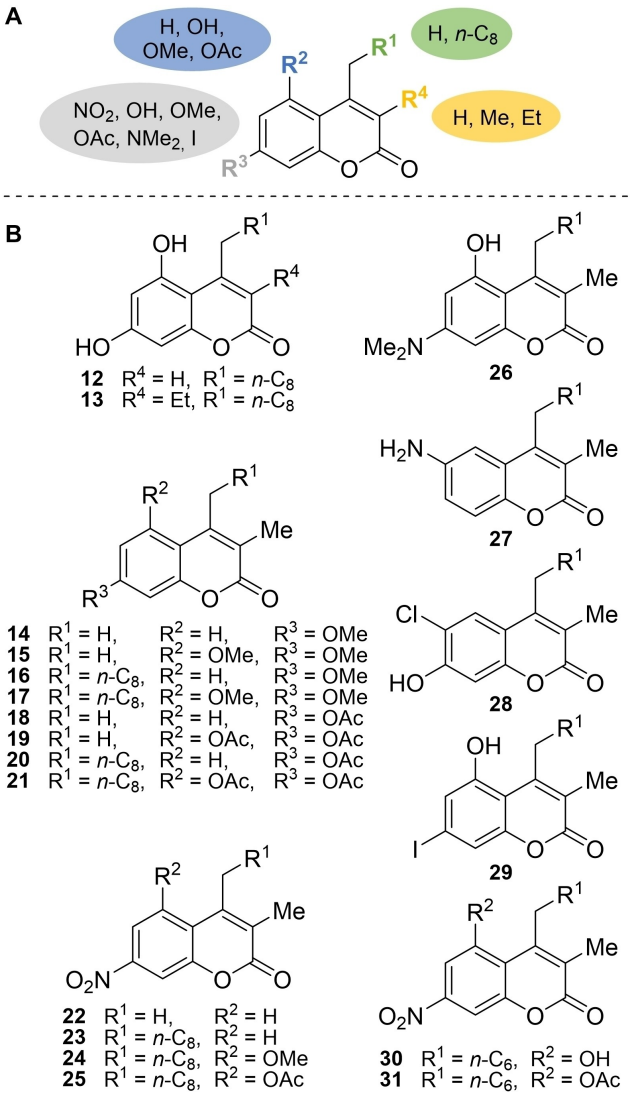

Figure 2. A. Structural changes introduced into the myxocoumarin scaffold in analogs **12–25**. **B.** Chemical structures of phenolic (**12**, **13**), *O*-methylated- (**14–17**) and *O*-acetylated- (**18–21**) myxocoumarin analogs, and further nitro myxocoumarins (**22–25**) as well as dimethylamino- (**26**), amino- (**27**), chloro- (**28**) and iodo- (**29**) substituted myxocoumarin analogs (for **26–29**, R^1 = *n*-C_8) and additional short-chain analogs **30** and **31**.

prospective applications of myxocoumarin B (**5**) thus remained elusive. This raised our interest in exploring potential other biological functions of **5**. We therefore set out to more broadly explore potential antimicrobial properties of myxocoumarin-type scaffolds within this work.

Initial screening of synthetic **5** against *Candida albicans*, *Pseudomonas aeruginosa*, *Escherichia coli*, *Enterococcus faecalis* and *Staphylococcus aureus* using classical disk-diffusion assays revealed a strong activity of **5** against the latter two, Gram-positive bacteria, comparable to the employed standard kanamycin. Owing to these promising preliminary results, a closer inspection of the antibiotic potential of the myxocoumarins was targeted. Given the straightforward and flexible synthetic access developed for **5**,[6] the preparation of a focused compound library to give first insights into structure-activity relationships across the myxocoumarin core was conducted. Of particular interest were variations at the prototypical myxocoumarin alkyl side chain to assess its role in granting antibacterial activity. Furthermore, the evaluation of analogs without the nitro substituent was of high interest, to exclude potential formation of non-specific toxic nitroso side products *in vivo*.[7] In addition, the synthesis of myxocoumarin derivatives lacking the nitro function is significantly simplified, giving very fast access to the target molecules.

The method of choice for the synthesis of myxocoumarin analogs was the condensation of β-keto esters with diverse alkyl substitution with phenol building blocks in a TFA-mediated Pechmann condensation.[8] Ethyl 2-methyl-acetoacetate (**6a**) was deprotonated with *n*-BuLi/DIPA and selectively alkylated with iodoalkanes **7b–k** to deliver the desired β-keto esters **6b–k** (Scheme 1). The analogs bearing linear side chains from C_4 to C_{11} (**6b–6i**) and C_{13} (**6j**) were obtained in yields ranging from 43% to 62%. The terminally branched **6k** gave a lower yield of 38%. The β-keto esters were subsequently condensed with resorcinol (**8**) and phloroglucinol (**9**) to give the corresponding mono- (**10a–k**) and dihydroxy (**11a–k**) myxocoumarin analogs (for yields, see Table 1).

To test the role of the methyl group at the position neighboring the ester functionality, derivatives bearing a proton (**12**) or an ethyl group (**13**) at R^4 were prepared by alkylation of

Table 2. Heat map of the antibacterial activity profile of myxocoumarin B (**5**) and its structural analogs **10**–**31** against *B. subtilis* NCTC5398, *S. aureus* NCTC6571, *S. aureas* MRSA compared to toxicity in zebrafish embryos. NCTC = National Collection of Type Cultures (NCTC, Culture Collection of Public Health, Salisbury, UK). Green color indicates antibiotic activity (darker green equals higher activity), organge color toxicity (darker orange equals higher toxicity).

Compound	*B. subtilis* NCTC5398 [μg/mL]	*S. aureus* NCT6571 [μg/mL]	*S. aureus* MRSA [μg/mL]	Zebrafish LC_{50} [μg/mL]
5	8	0.3	0.6	119.6
10a	>250	>250	>250	8.9
10b	31.2	62.5	62.5	2.1
10c	200	200	200	2.5
10d	200	200	200	1.5
10e	2	2	2	2.7
10f	15.6	7.8	7.8	21.5
10g	2	3.9	7.8	>151.2
10h	7.8	>250	250	30.5
10i	62.5	>250	>250	>82.6
10j	>250	>250	>250	>89.6
10k	15.6	>250	>250	5.2
11a	125	125	62.5	14.7
11b	15.6	15.6	15.6	9.0
11c	7.8	7.8	7.8	5.2
11d	7.8	4	2	4
11e	7.8	2.5	4	24.3
11f	4	15.6	7.8	>152.2
11g	31.2	7.8	31.2	>159.2
11h	>250	250	250	>158.2
11i	>250	>250	>250	>173.2
11j	>250	>250	>250	>187.3
11k	250	10	10	10.9
12	250	100	100	>250
13	5	12.5	50	>250
14	>250	>250	>250	12.7
15	>250	>250	>250	1.3
16	250	>250	>250	>158.2
17	62.5	>250	>250	>166.2
18	250	>250	>250	18.4
19	125	>250	>250	11.3
20	15.6	31.2	15.6	118.9
21	31.2	31.2	62.5	180.2
22	>250	>250	>250	25.8
23	>250	>250	>250	>165.7
24	>250	>250	>250	>180.7
25	0.3	0.15	0.15	27.8
26	>250	>250	>250	>172.7
27	>250	>250	>250	21.5
28	125	250	>250	>168.4
29	62.5	>250	250	67.6
30	2	0.3	0.3	20.2
31	1	0.15	1.25	18.6
Vancomycin	0.4	0.8	0.5	>250
Linezolid	0.8	3.1	3.1	>250

ethyl acetoacetate or ethyl 2-ethylacetoacetate with **7g** followed by Pechmann condensation with phloroglucinol (**9**).

To further increase the structural diversity of the myxocoumarin chemical library beyond hydroxyl analogs of **5**, a selection of *O*-methylated (**14**–**17**) and *O*-acetylated (**18**–**21**) derivatives was additionally prepared (Figure 2), either bearing a proton at position R^1 or an *n*-C_8 alkyl chain as in the original myxocoumarin scaffold. While compounds **14** and **18**–**21** were obtained by either *O*-methylation or *O*-acetylation of the corresponding phenol analogs **10a** and **10a**, **11a**, **10g**, **11g** using MeI or Ac_2O, respectively, **15**–**17** were generated by Pechmann condensation of 3,5-dimethoxyphenol or 3-methoxyphenol with either **6a** or **6g**. Furthermore, four myxocoumarin derivatives **22**–**25** bearing the natural nitro function were prepared. Compounds **22**–**24** were accessed by triflation and a subsequent nitration reaction of the corresponding hydroxy coumarins,[6] while **25** was synthesized by *O*-acetylation of myxocoumarin B (**5**). In addition, a dimethylamino- (**26**), amino- (**27**), chloro- (**28**) and iodo- (**29**) analog were accessed by Pechmann condensation of the correspondingly functionalized phenols with **6g** (see Supporting Information for experimental details on the syntheses of **12**–**29**).

Having this myxocoumarin library composed of the natural product **5** and 40 synthetic structural analogs in hands, we set out to evaluate their antimicrobial potential. All compounds were inactive against the opportunistic pathogenic yeast *C. albicans*, the gram-negative bacterium *Pseudomonas aeruginosa*, as well as the gram-positive *Micrococcus luteus* and *Listeria monocytogenes* at the maximum tested concentrations (250 μg/mL). However, strong antibacterial potential against the gram-positive bacteria *Bacillus subtilis* NCTC5398 and *S. aureus* NCTC6571 was observed for a number of analogs (Table 2, see Table S1). The natural product **5** exhibited very strong antibacterial activity against these test strains, with MIC values as low as 0.3 μg/mL against *S. aureus* NCTC6571 combined with an up to 400-fold higher LC_{50} value in a zebrafish model (119.6 μg/mL). For the mono-hydroxylated **10** and dihydroxylated **11** compound series, a clear structure-activity relationship became obvious, with the activity correlating with the length of the alkyl side chain at R^1. Considering the activity of analogs **10** against *S. aureus* NCTC6571, strong effects were only observed for **10e**–**g** with C_7 to C_9 alkyl substitution, with lowest MICs for the natural C_9 substituent. Inhibition of *B. subtilis* followed a similar trend, but activity extended to C_{10} and to a smaller extent to C_{11} substitution. The series of dihydroxylated analogs generally had a broader activity profile in terms of alkyl chain length, with significant inhibition already starting from C_4 up to C_9 substitution.

Alkyl chain lengths beyond the natural C_9 substituent lead to a fast drop in antibacterial activity for both compound series, **10** and **11**. When correlating antibacterial structure-activity relationships with toxicity in the zebrafish model, it became evident that longer side chains also lead to drastically increased LC_{50} values and thus less toxicity. Overall, besides the natural product **5**, **10f** (C_8), **10g** (C_9) and **11e**–**11g** (C_7-C_9) exhibited the most promising activity profiles.

When considering R^4 substitution, analog **12** bearing a proton at this position had dramatically reduced activity when compared to its methylated congener **11g**, while activity in ethyl derivative **13** was retained. Among all other tested compounds **14**–**29**, the *O*-acetylated analogs **20** and **21** and to an even lesser extent *O*-methylated derivative **17** and chlorinated **28** all bearing the natural C_9 alkyl substitution, retained weak antibacterial effects. Interestingly, the antibacterial activity of the *O*-acetylated analog **25** of myxocoumarin B (**5**) was approx. 25-fold higher against *B. subtilis* NCTC5398 and 2–4-fold higher against *S. aureus* when compared to the natural product. However, this was accompanied with an approx. 4-fold increase

Table 3. Antibiotic activity profile of **5**, **25** and **11 e** against a selection of *S. aureus* strains and *Enterococcus* sp. (top), including clinical isolates (bottom, strains isolated and identified from the clinical specimens delivered to veterinary Laboratory "VetLab", Belgrade, Serbia including dog urine, mouth and ear swab).

Compound	*S. aureus* MRSA ATCC43300 [μg/mL]	*S. aureus* ATCC9144 [μg/mL]	*Enterococcus faecium* ATCC6057 [μg/mL]
5	0.6	0.3	2
25	0.15	0.15	0.6
11 e	4	2.5	2.5
Compound	*Staphylococcus* sp. 80103770	Staphylococcus sp. 80100861	*Staphylococcus* sp. 80100865
5	0.3	0.3	2
25	0.15	0.15	0.6
11 e	2.5	5	2.5

in toxicity in the zebrafish model, overall leading to similar activity versus toxicity ratios.

Overall, these generated structure-activity data indicated that substitution at R^2 is required for strong antibiotic activity, preferably with OH or OAc, that analogs with nitro substitution at R^3 generally show higher activity (roughly 10-fold when compared to the respective phenolic derivatives), and that alkyl side-chain lengths from C_7 to C_9 seem to be optimal for activity, with increased side-chain lengths correlating with decreased toxicity in the zebrafish model. This structure-activity correlation was corroborated by synthesis of the C_7 analogs of **5**, without (**30**) and with (**31**) *O*-acetylation of the phenol at R^2. Both compounds indeed showed activity comparable to that of **5**, yet with approx. 6-fold increased toxicity. Most importantly, the antibacterial potential of all active myxocoumarin analogs was also retained against *S. aureus* MRSA, showing the high potential of these compounds to combat this clinically relevant, highly resistant bacterial pathogen.

We next evaluated the cytotoxicity of all myxocoumarin analogs with significant antimicrobial activity (at least one MIC value at or below 15.6 μg/mL) by screening against healthy human MRC-5 fibroblast cells (see Table S2). This revealed low selectivity indices (SI) for some derivatives (e.g., below 1 for **11 g** and **17**), with up to an SI of 87.5 for the natural product **5**. For further in-depth studies, we selected three analogs with high antibacterial activity combined with a range of selectivity indices, namely myxocoumarin B (**5**) (SI = 87.5), its *O*-acetyl analog **25** (SI = 25), and the most potent dihydroxylated congener **11 e** equipped with a C_7 alkyl chain (SI = 3.8). These compounds were evaluated against a larger panel of *S. aureus* strains, including clinical isolates (Table 3). The strains were collected from veterinary specimens (dog urine, ear swab and mouth swab) and showed resistance to one or more commonly used antibiotics in veterinary practice. *Enterococcus faecium*, as another Gram-positive opportunistic pathogen, was also included in the assessment. To our delight, all compounds showed pronounced antibacterial effects against all tested strains, with **25** being the most active antibacterial across all evaluated organisms (Table 3).

The likelihood of resistance development against **5**, **25** and **11 e** was assessed by multistep resistance selection of *S. aureus* ATCC9144 by propagating cultures with subinhibitory concentrations of the respective individual compound for 20 rounds, followed by one round of growth without selective pressure.[9] Over the course of this treatment, *S. aureus* developed a 5-fold increase in MIC against **5**, a 4-fold increase against **25** and only a 2-fold increase for **11 e**. Therefore, high antibiotic potential was retained for all compounds. This indicates a low likelihood of *S. aureus* for developing rapid resistance to the tested myxocoumarins.

Based on above resistance development assays and SI values, **5** and **25** were selected for evaluation of the antibiotic potential *in vivo* in a *S. aureus*- zebrafish infection model (Figure 3). The zebrafish infection model is a well-recognized platform for studying host-pathogen interactions, as well as for the development of therapeutic strategies.[10] In this experiment, wild type zebrafish embryos were challenged with the lethal systemic infection with *S. aureus* MRSA 43300, and followed for the survival and bacterial burden after 3-days treatments with **5** and **25**. Antibacterial efficacy of the selected myxocoumarins was evaluated in relation to the efficacy of vancomycin and linezolid, two antibiotics of clinical relevance. Analyses of zebrafish embryo survival coupled with bacterial proliferation confirmed that both compounds are highly efficient in rescuing zebrafish from infection, with the effect being dose dependent (Figure 3 A, B). Remarkably, both **5** and **25** proved approx. 10-fold more efficient at 0.5×MIC, with even approx. 35-fold increased activity at 1×MIC when compared to vancomycin, and approx. 2-fold higher activity at these concentrations when compared against linezolid.

Using 2×MIC of either **5** or **25** completely eliminated bacterial infection *in vivo*, as reflected in the efficiency of reduction of the bacterial burden (Figure 3C). Most importantly, treatment of infected zebrafish with **5** restored survival rates at all tested concentrations to the level of uninfected specimen (Figure 3A), thus proving both, high antibiotic efficiency and low toxicity of this compound upon application *in vivo*.

Overall, our work provides first structure-activity relationship data on a new class of antibiotics based on the myxocoumarin scaffold. It is interesting to note that the natural nitro substitution seems to be crucial for strong antibiotic activity. The most potent congeners provide outstanding sub-nanomolar antibacterial potency, even against drug-resistant *S. aureus* strains accompanied with low toxicity, both, *in vitro* and *in vivo*. Particularly encouraging are the obtained results on eliminating bacterial *S. aureus* infections in zebrafish by **5**, clearly outcompeting the established antibiotics vancomycin and linezolid, not only in terms of clearing infections, but most importantly also in terms of restoring survival of infected zebrafish to levels of healthy specimen. The myxocoumarins thus represent a valuable scaffold for the development of new antibiotics against clinically relevant bacterial pathogens, particularly for desperately needed new treatment option against MRSA.[11]

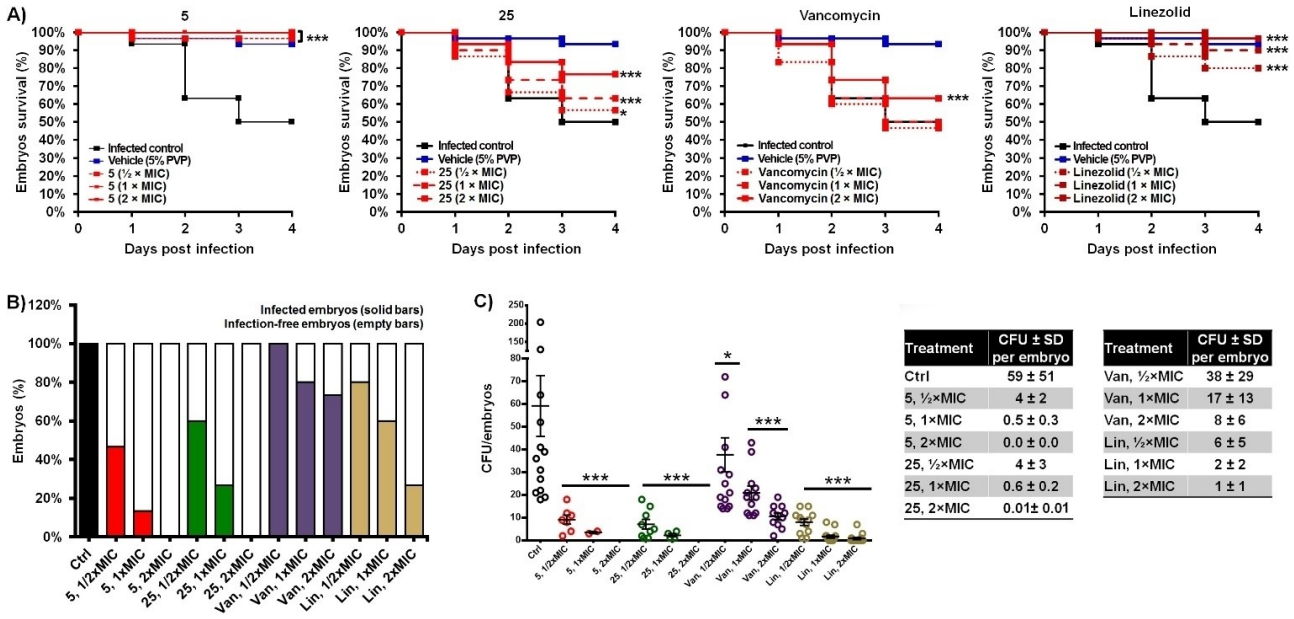

Treatment	CFU ± SD per embryo
Ctrl	59 ± 51
5, ½×MIC	4 ± 2
5, 1×MIC	0.5 ± 0.3
5, 2×MIC	0.0 ± 0.0
25, ½×MIC	4 ± 3
25, 1×MIC	0.6 ± 0.2
25, 2×MIC	0.01± 0.01

Treatment	CFU ± SD per embryo
Van, ½×MIC	38 ± 29
Van, 1×MIC	17 ± 13
Van, 2×MIC	8 ± 6
Lin, ½×MIC	6 ± 5
Lin, 1×MIC	2 ± 2
Lin, 2×MIC	1 ± 1

Figure 3. Myxocoumarin B (**5**) and derivative **25** rescued zebrafish embryos of *S. aureus* MRSA 43300 infection (A–B) and significantly decreased the bacterial burden (C). The Kaplan-Meier curves of the infected embryos survival upon different doses of vancomycin (Van), linezolid (Lin) and myxocoumarins **5** and **25** are shown. Survival of the treated infected fish was compared to those in the group without treatment (infected control) and the uninfected group (injected with 5% PVP [polyvinylpyrrolidone], which was used as a vehicle for the *S. aureus* suspension for infection). Embryos were monitored daily for survival. Data are compilations of two independent experiments using two replicates (n = 20 embryos/replicates) for each group. Bacterial burden was determined at 4 dpi by plating of the crushed embryos for colony forming units (CFUs). Data are compilations of two independent experiments using ten embryos for each group. Each dot represents an individual fish (square – untreated embryos, circle – treated embryos). The mean CFUs ± SEM are shown.

Acknowledgements

This work was generously funded by the German Research Foundation (DFG GU 1233/1-1) and by the Ministry of Education, Science and Technological Development of the Republic of Serbia (agreement no. 451-03-68/2020-14/200042) and DAAD (Deutscher Akademischer Austauschdienst, Bilateral Project of Germany with the Republic of Serbia to SV and TAMG – 2020/2021). Open Access funding enabled and organized by Projekt DEAL.

Conflict of Interest

The authors declare no conflict of interest.

Data Availability Statement

The data that support the findings of this study are available in the supplementary material of this article.

Keywords: antibiotics · myxocoumarins · natural products · *Staphylococcus aureus* · structure-activity relationships

[1] a) T. F. Schäberle, F. Lohr, A. Schmitz, G. M. König, *Nat. Prod. Rep.* **2014**, *31*, 953–972; b) J. Herrmann, A. Abou Fayad, R. Müller, *Nat. Prod. Rep.* **2017**, *34*, 135–160; c) K. Gemperlein, N. Zaburannyi, R. Garcia, J. J. La Clair, R. Müller, *Mar. Drugs* **2018**, *16*, 314–329; d) C. D. Bader, F. Panter, R. Müller, *Biotechnol. Adv.* **2020**, *39*, 107480.
[2] a) D. M. Bollag, P. A. McQueney, J. Zhu, O. Hensens, L. Koupal, J. Liesch, M. Götz, E. Lazarides, C. M. Woods, *Cancer Res.* **1995**, *55*, 2325–2333; b) K. Gerth, N. Bedorf, G. Höfle, H. Irschik, H. Reichenbach, *J. Antibiot.* **1996**, *49*, 560–563; c) H. Reichenbach, G. Höfle, *Drugs* **2008**, *9*, 1–10.
[3] a) K. Gerth, N. Bedorf, H. Irschik, G. Höfle, H. Reichenbach, *J. Antibiot.* **1994**, *47*, 23–31; b) A. Naini, F. Sasse, M. Brönstrup, *Nat. Prod. Rep.* **2019**, *36*, 1394–1411.
[4] a) S. Baumann, J. Herrmann, R. Raju, H. Steinmetz, K. I. Mohr, S. Hüttel, K. Harmrolfs, M. Stadler, R. Müller, *Angew. Chem. Int. Ed.* **2014**, *53*, 14605–14609; *Angew. Chem.* **2014**, *126*, 14835–14839; b) S. Hüttel, G. Testolin, J. Herrmann, T. Planke, F. Gille, M. Moreno, M. Stadler, M. Brönstrup, A. Kirsching, R. Müller, *Angew. Chem. Int. Ed.* **2017**, *56*, 12760–12764; *Angew. Chem.* **2017**, *129*, 12934–12938.
[5] T. A. M. Gulder, S. Neff, T. Schütz, T. Winkler, R. Gees, B. Böhlendorf, *Beilstein J. Org. Chem.* **2013**, *9*, 2579–2585.
[6] J. I. Müller, K. Kusserow, G. Hertrampf, A. Pavic, J. Nikodinovic-Runic, T. A. M. Gulder, *Org. Biomol. Chem.* **2019**, *17*, 1966–1969.
[7] a) K. Nepali, H.-Y. Lee, J.-P. Liou, *J. Med. Chem.* **2019**, *62*, 2851–2893; b) V. Purohit, A. K. Basu, *Chem. Res. Toxicol.* **2000**, *13*, 673–692.
[8] a) H. v. Pechmann, *Ber. Dtsch. Chem. Ges.* **1884**, *17*, 929–936; b) M. Katkevičs, A. Kontijevskis, I. Mutule, E. Sūna, *Chem. Heterocycl. Compd.* **2007**, *43*, 151–159.
[9] D. J. Farrell, M. Robbins, W. Rhys-Williams, W. G. Love, *Antimicrob. Agents Chemother.* **2011**, *55*, 1177–1181.
[10] a) V. Torraca, S. Mostowy, *Trends Cell Biol.* **2018**, *28*, 143–156; b) C. Medina, J. L. Royo, *Methods* **2013**, *62*, 241–245; c) Y.-J. Li, B. Hu, *J. Genet. Genomics* **2012**, *39*, 521–534.
[11] S. Cascioferro, D. Carbone, B. Parrino, C. Pecoraro, E. Giovannetti, G. Cirrincione, P. Diana, *ChemMedChem* **2020**, *16*, 65–80.

Manuscript received: February 8, 2022
Accepted manuscript online: March 1, 2022
Version of record online: April 26, 2022